NBSIR 73-325

# PULSE TESTING OF RF AND MICROWAVE COMPONENTS

William L. Gans and N. S. Nahman

Electromagnetics Division
Institute for Basic Standards
National Bureau of Standards
Boulder, Colorado 80302

July 1973
Interim Report

Prepared for:
Department of Defense
Calibration Coordination Group
72-68

NBSIR 73-325

# PULSE TESTING OF RF AND MICROWAVE COMPONENTS

William L. Gans and N.S. Nahman

Electromagnetics Division
Institute for Basic Standards
National Bureau of Standards
Boulder, Colorado 80302

July 1973
Interim Report

Prepared for:
Department of Defense
Calibration Coordination Group
72-68


U.S. DEPARTMENT OF COMMERCE, Frederick B. Dent, Secretary

NATIONAL BUREAU OF STANDARDS. Richard W Roberts. Director

CONTENTS

LIST OF FIGURES

List of Figures (Con't)

## ABSTRACT

This interim report is concerned with the application of time domain measurements to the determination of frequency domain parameters. The theory is developed for the calculation of the parameter $S_{21}(\omega)$ from time domain insertion measurements. Experimental results are presented for a 4.1 GHz low pass filter and coaxial attenuators of 10 dB, 20 dB and 40 dB. Also presented is an experimental justification showing the lack of feasibility of applying time domain techniques to the frequency response calibration of certain ac VTVMs.



Key Words: Fast fourier transform; frequency response; microwave; pulse; S-parameter; time domain; transfer function.

# 1. INTRODUCTION

This report is an interim report to the sponsor containing a condensed description of work accomplished through fiscal 1973. Upon completion of the overall project objective a comprehensive final report shall be published. The overall project objective is to develop the capability at NBS to rapidly measure and process time domain data such that new advances in time domain instrumentation can be accurately and efficiently analyzed.

Specifically, this interim report is concerned with the application of time domain measurements to the determination of frequency domain parameters as functions of frequency. Such an application of time domain measurements is intimately related to the processing of time domain pulse data.

The report is divided into three chapters, the first being the present introduction. Chapter 2 of this report contains the development of a model used for the computation of the frequency domain parameter $S_{21}(s)$ from time domain measurements. In addition, this chapter contains the description and results of experimental time domain insertion measurements for a coaxial low-pass filter and three coaxial attenuators. $S_{21}(j\omega)$ is computed for each component.

Chapter 3 consists of a description of experiments using both frequency domain and time domain techniques aimed at determining the feasibility of calibration of certain ac VTVM's using time domain measurement methods. The conclusion drawn from these experiments is that although time domain techniques are quite powerful, their use for this purpose is unfeasible.

## 2. COAXIAL MICROWAVE DEVICE EXPERIMENT

The general goal of this experiment was to determine the frequency response characteristics of four coaxial microwave devices from measured time domain data.[1]. The commercial devices tested were a 4.1 GHz low pass filter, a 10 dB attenuator, a 20 dB attenuator and a 40 dB attenuator.

### 2.1 Theory

These measurements were actually time domain insertion loss measurements for the computation of the transfer insertion parameter, $S_{21}(j\omega)$, where $\omega$ is the angular frequency variable. [2]. A circuit model analysis justifying the experimental measurement technique now follows.

The circuit used to obtain the incident voltage waveform at the plane of insertion is shown in Figure 2-1. $E_g(s)$ and $Z_g(s)$ represent the voltage source transition waveform generator where $s$ is the complex frequency variable. $\ell_1$, $\ell_2$, and $\ell_3$ are three sections of precision coaxial airline of impedance $R_o$. The box labeled T(s) represents the sampling oscilloscope with an input impedance of Z(s) across the line and a transfer function T(s). $e_{d1}(t)$ is an observable voltage; it is the insertion plane transition waveform as seen through the transfer properties of $\ell_2$ and the oscilloscope. $Z_T(s)$ is a termination whose impedance is very close to $R_o$. For this analysis, it is assumed that all connectors are ideal.

Since the generator impedance, $Z_g(s)$, may not be equal to $R_o$, and since the presence of the sampling oscilloscope at the end of line $\ell_2$ certainly changes the load impedance as seen by line $\ell_2$ to some value other than $R_o$, the reflections caused by these two discontinuities

will invalidate this analysis after some time $\tau$. The available time window in which this measurement is valid is determined by the lengths of the two lines, $\ell_1$ and $\ell_2$. The time delays for reflections from the generator and the oscilloscope, respectively, are

$$\tau_1 = 2\ell_1\sqrt{LC}$$
$$\tau_2 = 2\ell_2\sqrt{LC} \quad . \tag{2-1}$$

Thus $\tau$, the available time window, will be either $\tau_1$ or $\tau_2$, which ever is smaller.

The displayed initial input transition voltage waveform, $e_{d1}(t)$, may be expressed as

$$e_{d1}(t) = \mathcal{L}^{-1}\{E_{d1}(s)\} \qquad 0 < t < \frac{\tau_1}{2} + \frac{\tau_2}{2} + \tau \tag{2-2}$$

where $\mathcal{L}^{-1}$ denotes the inverse Laplace transformation operator, and where $E_{d1}(s)$ is given in terms of the complex frequency variable $s$ as

$$E_{d1}(s) = E_g(s)\left\{\frac{R_o e^{-s(\ell_1+\ell_2)\sqrt{LC}}}{Z_g(s)+R_o}\right\}\left\{\frac{\dfrac{Z(s)R_o}{Z(s)+R_o}}{R_o+\dfrac{Z(s)R_o}{Z(s)+R_o}}\right\}T(s) \quad . \tag{2-3}$$

For purposes of clarity and precision, the word "initial" used above refers to the waveform present at the insertion plane only during the inverval 0 to $\frac{\tau_1}{2} + \tau$. If the generator and load impedances were both equal to the line impedance $R_o$, then one could refer to the waveform at the insertion plane as an "incident" waveform, the distinction being that the incident waveform would exist over the time interval $(o, \infty)$. By using two different terms, a clearer distinction is made between the generator waveform over all time, and that part of the generator waveform undistorted by reflections from either the source or the oscilloscope impedance discontinuities within the time window. Furthermore, the term "initial" can be used to describe waves arriving or departing from a given port. For example, $E_{1i}(s)$ is the initial waveform arriving at the insertion plane while $E_{2t}(s)$ will designate the initial waveform departing (or transmitted) from the output port of the network under test.

Writing (2-3) in terms of $E_{1i}(s)$,

$$E_{d1}(s) = E_{1i}(s) \left\{ \frac{\frac{Z(s)\ R_o}{Z(s) + R_o}}{R_o + \frac{Z(s)\ R_o}{Z(s) + R_o}} \right\} T(s)\ e^{-s\ \ell_2 \sqrt{LC}} . \qquad (2\text{-}4)$$

Referring to Figure 2-2, with the addition of the device under test into the 50 ohm system, the initial transmitted voltage waveform $E_{2t}(s)$ may be expressed in the complex frequency plane as

$$E_{2t}(s) = E_{1i}(s)\ S_{21}(s) . \qquad (2\text{-}5)$$

The displayed initial transmitted voltage waveform $e_{d2}(t)$ is

$$e_{d2}(t) = \mathcal{L}^{-1}\{E_{d2}(s)\} \quad o < t < \frac{\tau_1}{2} + \frac{\tau_2}{2} + \tau_d + \tau \qquad (2\text{-}6)$$

where

$$E_{d2}(s) = E_{2t}(s) \left\{ \frac{\dfrac{Z(s)\,R_o}{Z(s)+R_o}}{R_o + \dfrac{Z(s)\,R_o}{Z(s)+R_o}} \right\} T(s)\, e^{-s\,\ell_2\sqrt{LC}} . \qquad (2\text{-}7)$$

$\tau_d$ is the additional time delay introduced by the device under test.
From equations (2-5) and (2-7) $E_{d2}(s)$ is given by

$$E_{d2}(s) = E_{1i}(s)\,S_{21}(s) \left\{ \frac{\dfrac{Z(s)\,R_o}{Z(s)+R_o}}{R_o + \dfrac{Z(s)\,R_o}{Z(s)+R_o}} \right\} T(s)\, e^{-s\,\ell_2\sqrt{LC}} . \qquad (2\text{-}8)$$

The quotient of $E_{d2}(s)$ and $E_{d1}(s)$ will yield the following result:

$$\frac{E_{d2}(s)}{E_{d1}(s)} = S_{21}(s) . \qquad (2\text{-}9)$$

Thus, for the two time domain waveforms actually observed, in terms of Laplace transforms,

$$S_{21}(s) = \frac{\mathcal{L}\{e_{d2}(t)\}}{\mathcal{L}\{e_{d1}(t)\}} \qquad (2\text{-}10)$$

or, replacing s by $j\omega$, we arrive at the final Fourier transform equation

$$S_{21}(j\omega) = \frac{F\{e_{d2}(t)\}}{F\{e_{d1}(t)\}} \quad . \qquad (2\text{-}11)$$

## 2.2 Experimental Test Setup

The basic test configuration consisted of a 20 ps. 10%-90% transition time voltage step generator, a 28 ps. 10%-90% transition time sampling oscilloscope and a 1000 point local digital memory. Precision 7 mm coaxial air lines were used for discontinuity reflection isolation. The available time window $\tau$ was 1 ns. The complete system block diagram is shown in Figure 2.3. [3].

With the device under test removed from the system, the time domain waveform from the tunnel diode pulse generator was sampled and recorded as a 1000-point waveform. The device under test was then placed in the line as shown in the block diagram and another 1000-point waveform was recorded. The first waveform, $e_{d1}(t)$ is the initial waveform in the 50 ohm system while the second waveform, $e_{d2}(t)$ is the initial transmitted waveform from the network under test.

Due to an excessive amount of noise in the system, some waveform signal averaging was necessary. This averaging was accomplished by taking several hundred voltage samples at each of the 1000 incremental time divisions. All the voltage samples taken at a given point in time were then averaged through a simple R-C averaging circuit and the resultant averaged voltage value was stored in memory.

This technique, in effect, is similar to averaging several hundred 1000-point time domain waveforms. The primary difference is that averaging is done prior to storage in memory, so that the required memory size is minimal.

Once the insertion waveforms were acquired and stored, they were punched onto teletype paper tape. These records were then read into an in-house computer where they were processed using a Fast Fourier transform (FFT) subroutine.

The output of this subroutine consists of a set of complex frequency domain coefficients for each transformed time domain waveform. The amplitude frequency response of the test devices may then be obtained by computing the ratio of the magnitude of the output and input frequency domain coefficients for each frequency point of interest.

The resulting amplitude frequency response characteristics for each device were then plotted as graphs of gain in dB versus frequency.

## 2.3 Experimental Data and Results

### 2.3.1 4.1 GHz Low Pass Filter

The 4.1 GHz low pass filter tested had a nominal impedance of 50 $\Omega$. It was equipped with type N connectors, one male and one female. Filter insertion loss was rated at $\leq$ 1 dB below .9 x cut off frequency and rejection was rated at $\geq$ 50 dB above 1.25 x cut off frequency. Figure 2.4 contains photographs of the insertion time domain waveforms obtained on the sampling oscilloscope. In this case, as well as the following three cases, the transmitted initial waveform, $e_{d2}(t)$, is delayed from the initial 50 ohm system waveform, $e_{d1}(t)$. Thus, in the photographs, the output waveform transition occurs to the right of the input waveform transition. The sampling oscilloscope was sampling

at a rate of 91.6 kHz. Figure 2.5 is a photograph of these same waveforms as observed on a monitor oscilloscope after signal averaging was done. These were the waveforms actually stored in local memory for computer processing.

Figure 2.6 is a computer plot of the frequency response of the low pass filter as calculated using the fast Fourier transform.

### 2.3.2 10 dB Coaxial Attenuator

The 10 dB attenuator tested was a dc to 18 GHz device with a rated maximum deviation from nominal attenuation of ± 0.5 dB. The connectors were both type N, one male and one female. The attenuator's nominal impedance was 50 Ω.

Figure 2.7 is a photograph of both input and output time domain waveforms as seen on the sampling oscilloscope. The sampling oscilloscope sampling repetition rate was 24 kHz. Figure 2.8 is a photograph of both waveforms after signal averaging. Figure 2.9 is a computer plot of the frequency response of the 10 dB attenuator.

### 2.3.3 20 dB Coaxial Attenuator

The 20 dB attenuator was the same type as the 10 dB attenuator. Figure 2.10 is a photograph of the unaveraged input and output waveforms. Figure 2.11 is a photograph of both waveforms after signal averaging. Figure 2.12 is a computer plot of the frequency response of the 20 dB attenuator.

### 2.3.4 40 dB Coaxial Attenuator

The 40 dB attenuator was, again, the same type as the 10 dB attenuator with the single exception that its rated maximum deviation from nominal attenuation was ± 1.0 dB.

Figure 2.13 is a photograph of the unaveraged input and output waveforms for the 40 dB attenuator. Figure 2.14 is a photograph of both averaged waveforms. Figure 2.15 is a computer plot of the frequency response of the 40 dB attenuator.

# 3. AC ELECTRONIC VOLTMETER MEASUREMENTS

## 3.1 Experimental Purpose

The purpose of this experiment was to determine the feasibility of utilizing time domain waveform measurement techniques for calibration of certain electronic ac voltmeters suitable for measurements in the 20 Hz to 4 MHz frequency range.

One particular model was selected to represent this class of test instrument and was subjected to both frequency domain and time domain testing. A simplified block diagram of the VTVM is shown in Figure 3-1.

Using twelve steps of attenuation, this meter measures ac voltage from 0.001 to 300 volts RMS full scale. The instrument is an RMS indicating, average responding voltmeter with a frequency bandwidth from 10 Hz to 4 MHz. Instrument accuracy varies from ± 1% to ± 5% of full scale, the larger errors appearing at the extreme low and high frequency regions of the rated bandwidth.

## 3.2 Frequency Domain Tests

In order to provide a basis for verification of the time domain tests which follow, frequency domain measurements of the VTVM's amplifier frequency response were first conducted. Figure 3-2 is a block diagram of the system used to perform these measurements.

Briefly, the measurements were conducted as follows. With the system set up as depiected in Figure 3-2, and with the VTVM attenuation switch set to 0.3 V full scle, the CW generator frequency was set at 500 kHz. The amplitude of the generator sine wave was then adjusted to 0.3 V as observed on the reference RF voltmeter. The voltage observed on the measurement voltmeter was then recorded.

This procedure was then repeated in steps of 200 or 300 kHz over the range of frequencies from 500 kHz to 12 MHz. A graph of the resulting VTVM amplifier frequency response scaled in dB versus frequency is shown in Figure 3-3.

Since the manufacturer of this particular VTVM states that the meter frequency response may vary as a function of the load impedance across the OUTPUT terminals, the entire measurement described above was repeated with the output termination removed. The results of this test, again in dB versus frequency, are shown in Figure 3-4.

The important feature to be noticed in both of these graphs is the -3 dB point; in both cases, the meter amplifier gain, as measured at the OUTPUT terminals, drops by 3 dB at approximately 9 MHz. The instrument as a whole, however, has a rated upper band limit of only 4 MHz. Thus, these measurements appear to indicate that the frequency response of the meter amplifier and frequency response of the whole instrument are not identical. This observation was substantiated by the fact that the meter needle indication indeed dropped rather abruptly as the test signal frequency increased above 4 MHz.

## 3.3 Time Domain Tests

The time domain tests conducted on the ac voltmeter were performed on the same system as was used in the microwave experiments described in Chapter 2. (See Figure 2-3). The only change to the system was the substitution of a lower speed (350 ps 10%-90% transition time ) sampling head for purposes of noise reduction.

As in Chapter 2, with the voltmeter removed from the system, the time domain waveform from a voltage step waveform generator was sampled and recorded as a 1000-point waveform. The voltmeter

was then inserted into the system, and the initial transmitted meter amplifier response waveform was sampled and recorded as another 1000-point waveform.

These two waveforms were then made periodic, smoothed and processed using a fast Fourier transform subroutine [4]. The meter amplifier response waveform, after being made periodic and smoothed, is shown in Figure 3-5. The meter amplifier frequency response was then plotted on an X-Y recorder in decibels versus frequency as shown in Figure 3-6.

Observation of this figure along with Figures 3-3 and 3-4 will reflect the close correlation between meter amplifier responses obtained by frequency domain and time domain techniques. As in the frequency domain case, the time domain techniques yielded a -3 dB point close to 9 MHz.

## 3.4 Conclusions

In Chapter 2, a method was derived to obtain time domain insertion data. Using the time domain data, $S_{21}(j\omega)$ was computed for several microwave devices. Although much work remains in the areas of pulse generation, oscillographic techniques and data acquisition and reduction, this method appears quite promising as a calibration technique.

On the other hand, the experiments conducted in Chapter 3 show quite decisively that time domain measurement techniques, like their frequency domain counterparts, cannot be applied blindly to all areas of frequency response measurements. In particular, the feasibility of using time domain techniques to measure the frequency response of this type of ac VTVM is considered poor.

Both the time domain and frequency domain data closely agree that the meter amplifier half power point lies near 9 MHz. However, the meter indication, as read from the meter face, drops rapidly above 4 MHz. It appears, then, that the network frequency response of the meter amplifier and the frequency response of the indicating meter itself are quite different. Although time domain calibration of the meter amplifier is feasible, there is no justification that the visually read meter would thus be calibrated. In short, there appears to be no reliable correlation between the meter amplifier frequency response and the visually read meter frequency response.

More generally, analog instruments that are visually read such as oscilloscopes and VTVM's, should be visually calibrated. Unless a repeatable and reliable correlation can be established between the instrument's visual indicator and measurable electronic properties, any attempt to calibrate the instrument by purely electronic means must be considered invalid.

## 4. REFERENCES


1. Nicholson, A. M., "Broad-Band Microwave Transmission Characteristics from a Single Measurement of the Transient Response", IEEE Trans. on Instrumentation and Measurement, Vol. IM-17, No. 4, pp. 395-402, December, 1968.

2. Ramo, S., J. R. Whinnery, and T. Van Duzer, Fields and Waves in Communication Electronics, John Wiley & Sons, New York, 1965, pp. 603-609.

3. Gans, W. L., "Block Diagrams, Schematic Circuit Diagrams, and Operating Instructions for the Time Domain Measurement System", NBSIR 73-321 (to be published).

4. Gans, W. L. and N. S. Nahman, "Fast Fourier Transform Implementation for the Calculation of Network Frequency Domain Transfer Functions from Time Domain Waveforms", NBSIR 73-303, December, 1972.

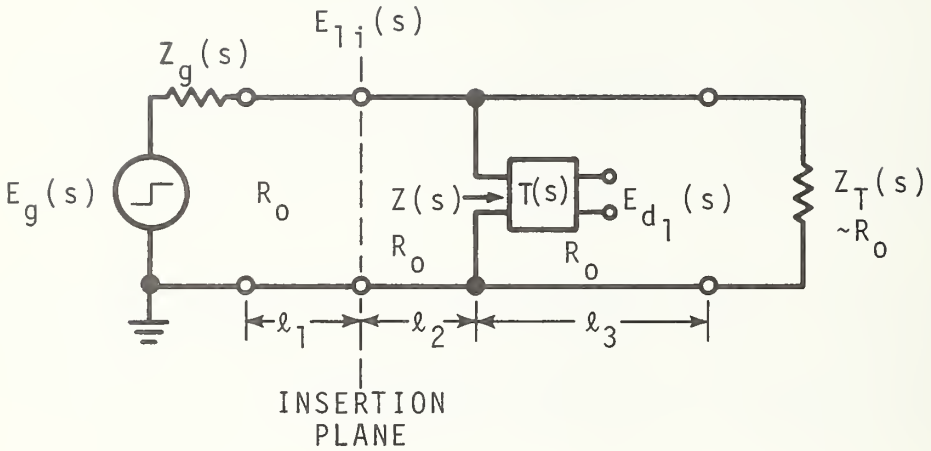


Figure 2-1. Diagram of circuit used to obtain $e_{d1}(t)$.

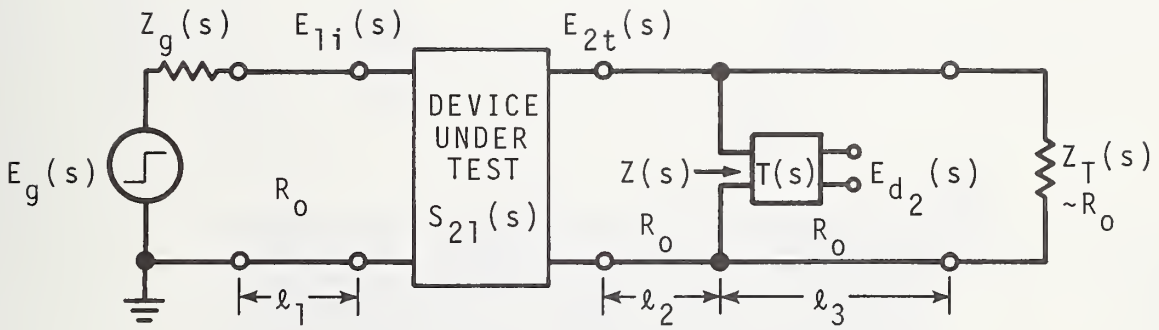


Figure 2-2. Diagram of circuit used to obtain $e_{d2}(t)$.

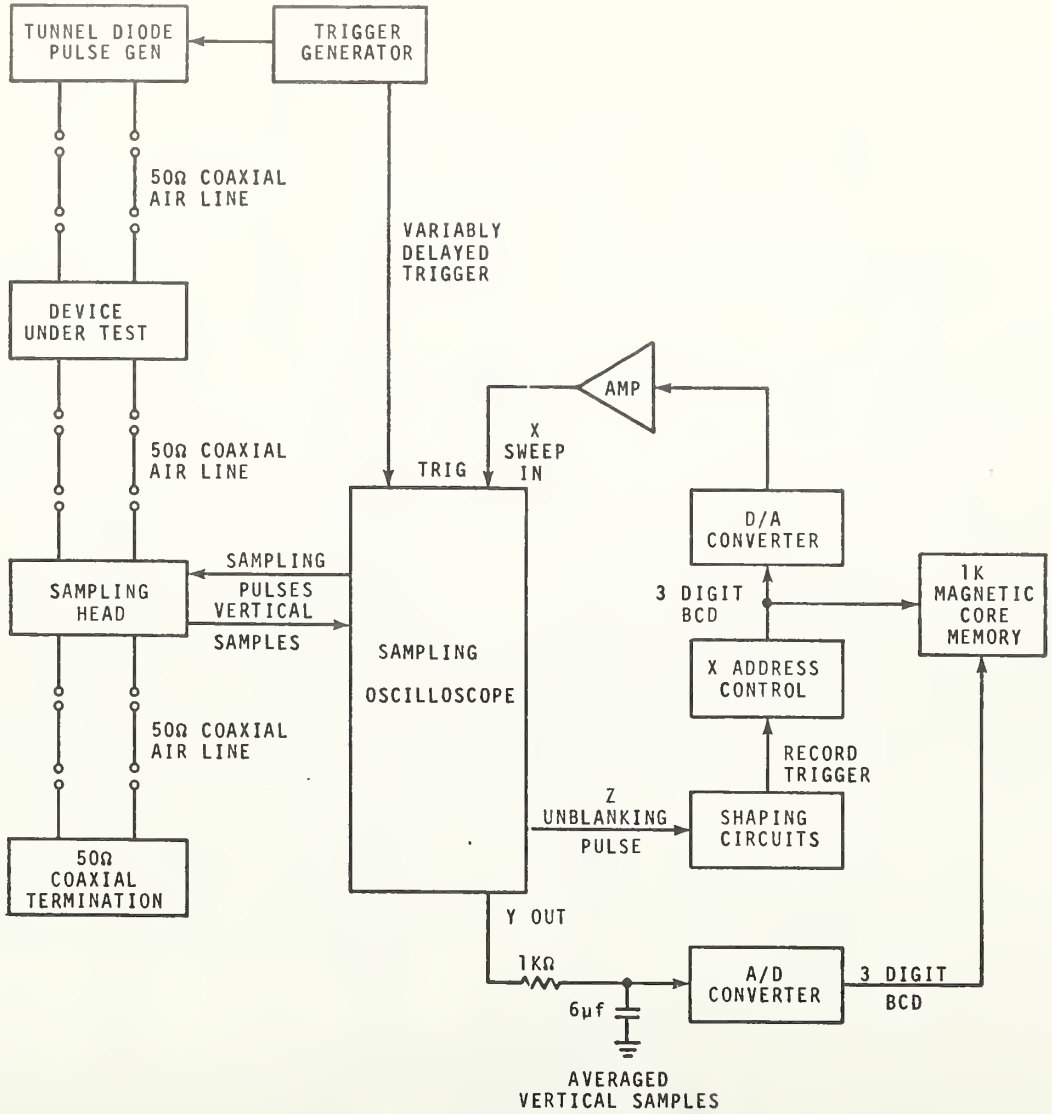


Figure 2-3. Complete time domain data acquisition system block diagram.

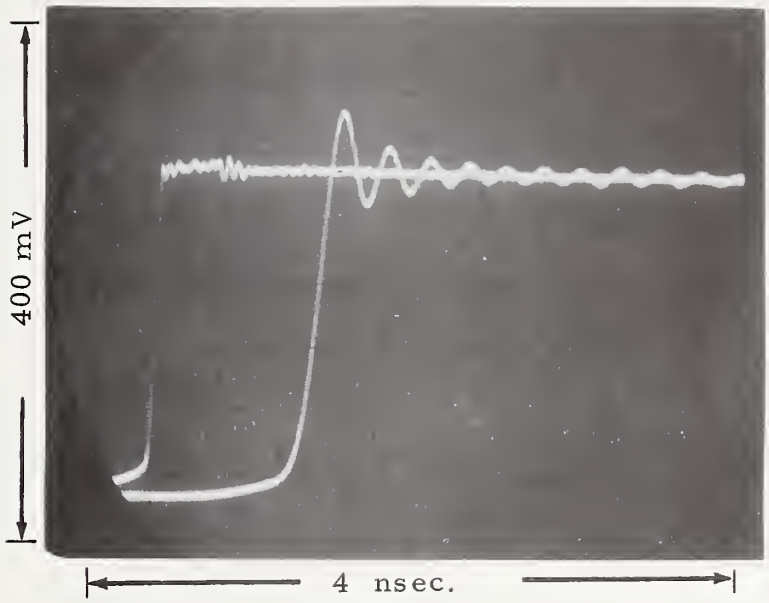


Figure 2-4. Photograph of $e_{d1}(t)$ and $e_{d2}(t)$ for the 4.1 GHz low pass filter as seen on the sampling oscilloscope.

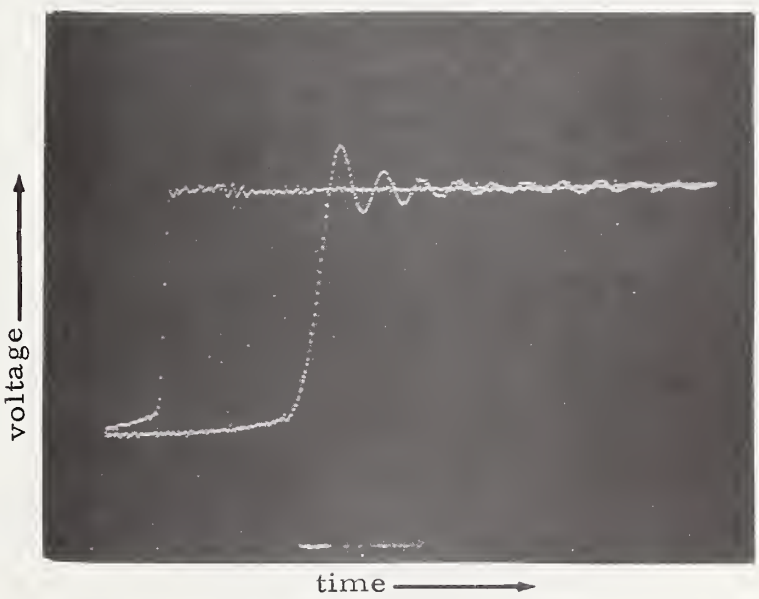


Figure 2-5. Photograph of $e_{d1}(t)$ and $e_{d2}(t)$ for the 4.1 GHz low pass filter after signal averaging.

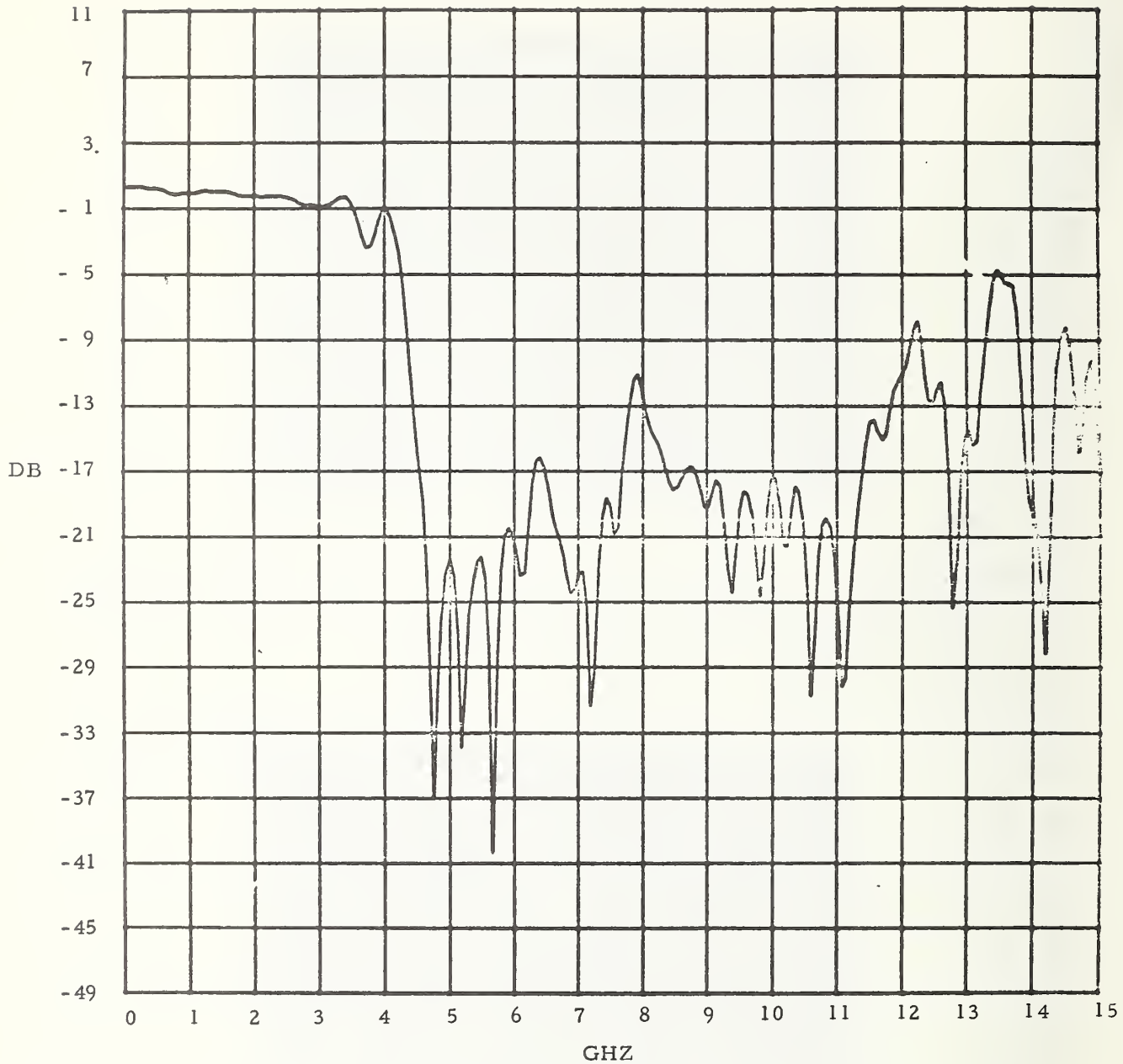


Figure 2-6. Computer plot of the amplitude frequency response of the 4.1 GHz low pass filter .

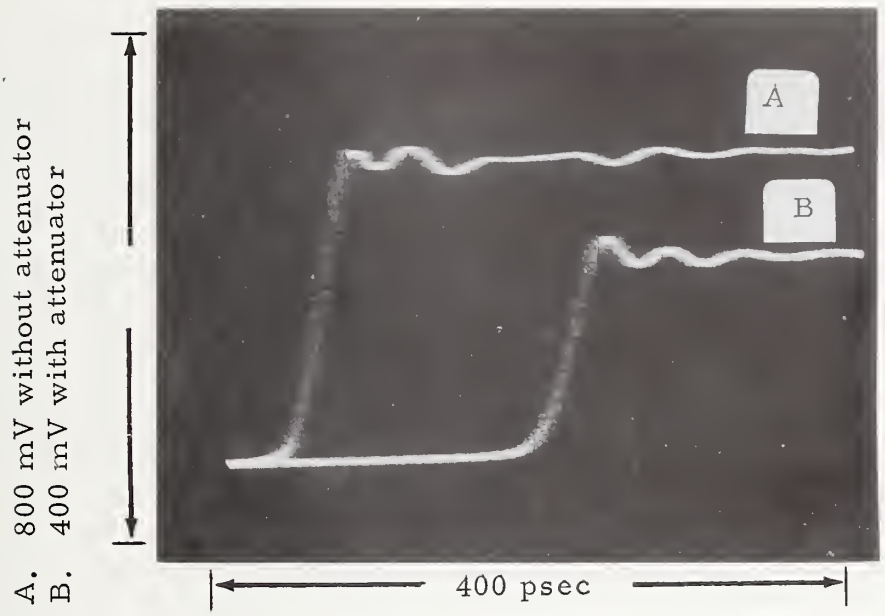


Figure 2-7. Photograph of $e_{d1}(t)$ and $e_{d2}(t)$ for the 10 dB attenuator as seen on the sampling oscilloscope.

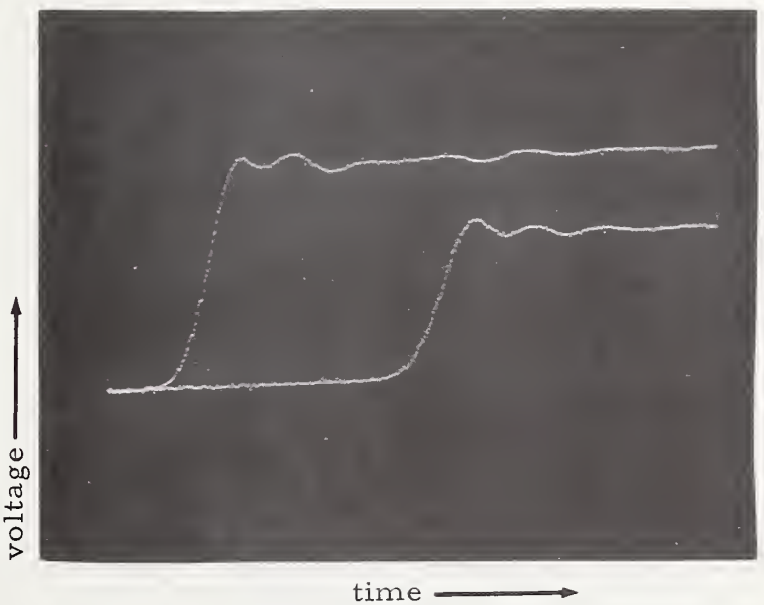


Figure 2-8. Photograph of $e_{d1}(t)$ and $e_{d2}(t)$ for the 10 dB attenuator after signal processing.

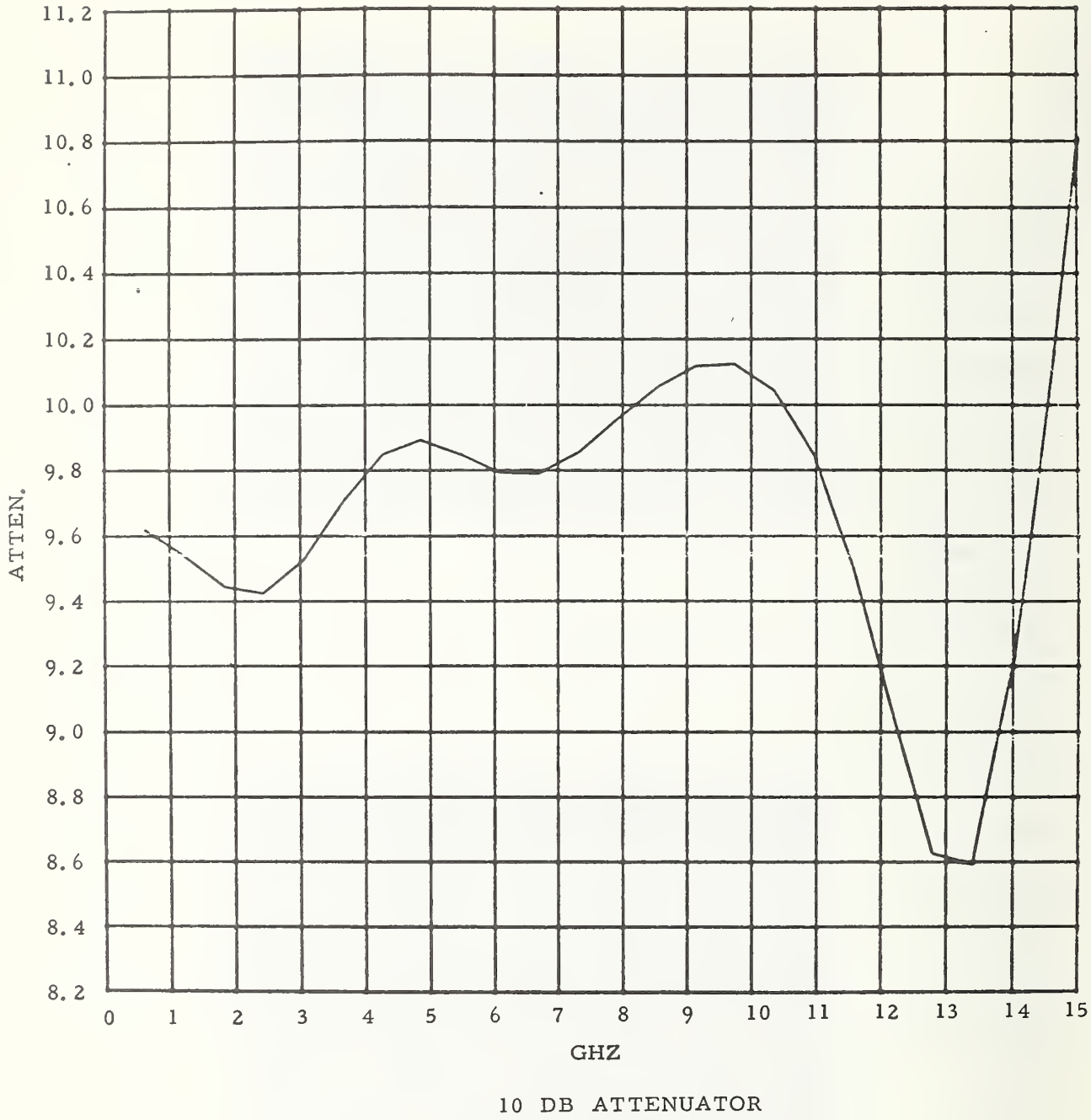


Figure 2-9. Computer plot of the amplitude frequency response of the 10 dB attenuator.

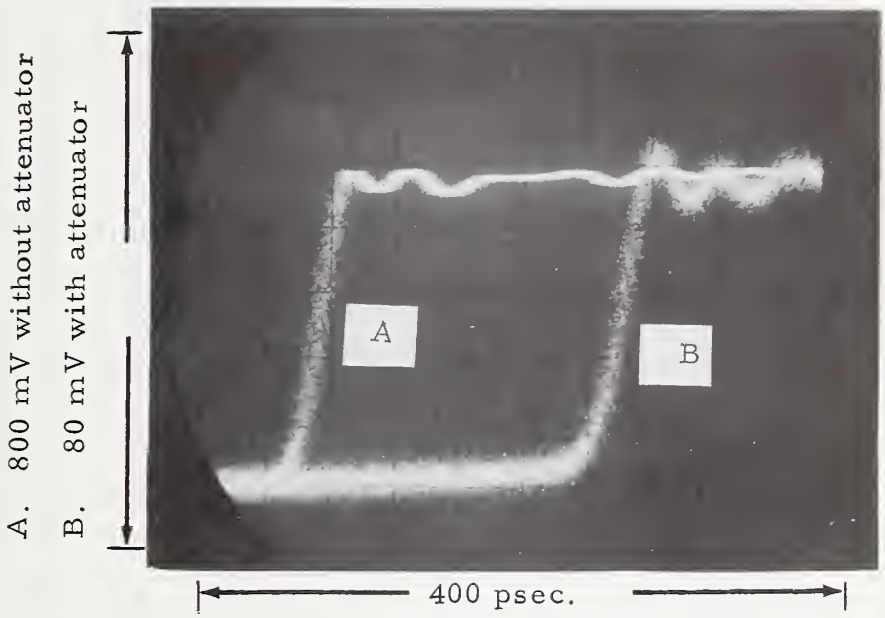


Figure 2-10. Photograph of the $e_{d1}(t)$ and $e_{d2}(t)$ for the 20 dB attenuator as seen on the sampling oscilloscope.

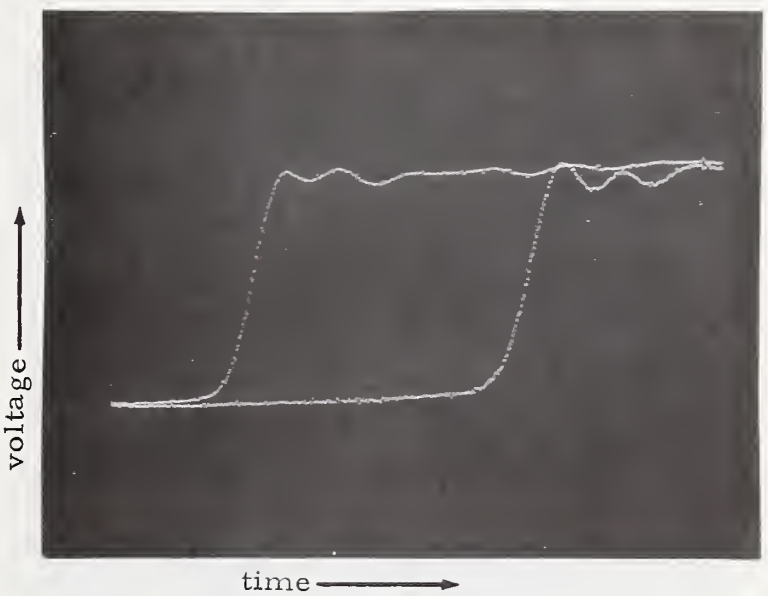


Figure 2-11. Photograph of $e_{d1}(t)$ and $e_{d2}(t)$ for the 20 dB attenuator after signal averaging.

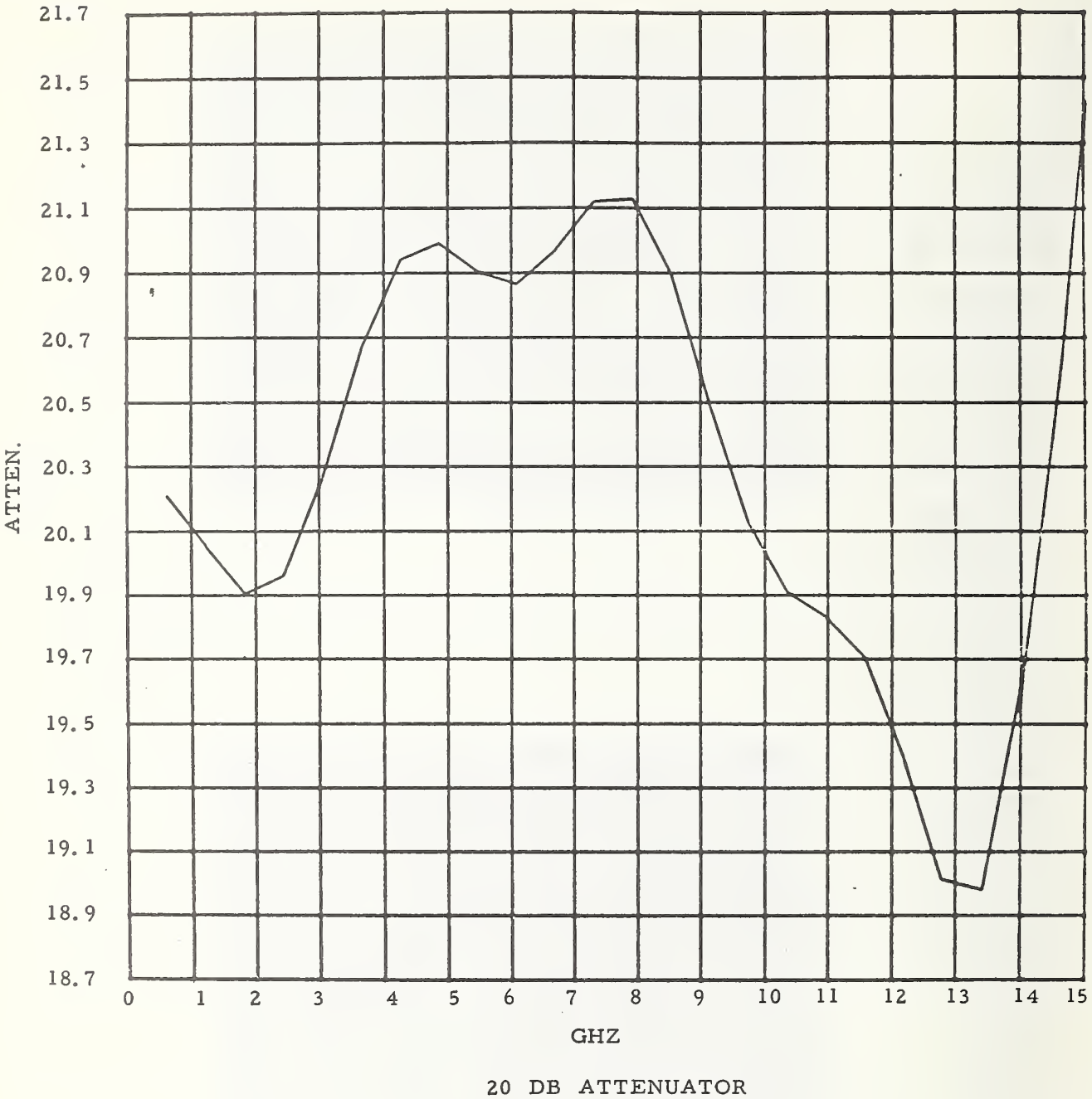


Figure 2-12. Computer plot of the amplitude frequency response of the 20 dB attenuator.

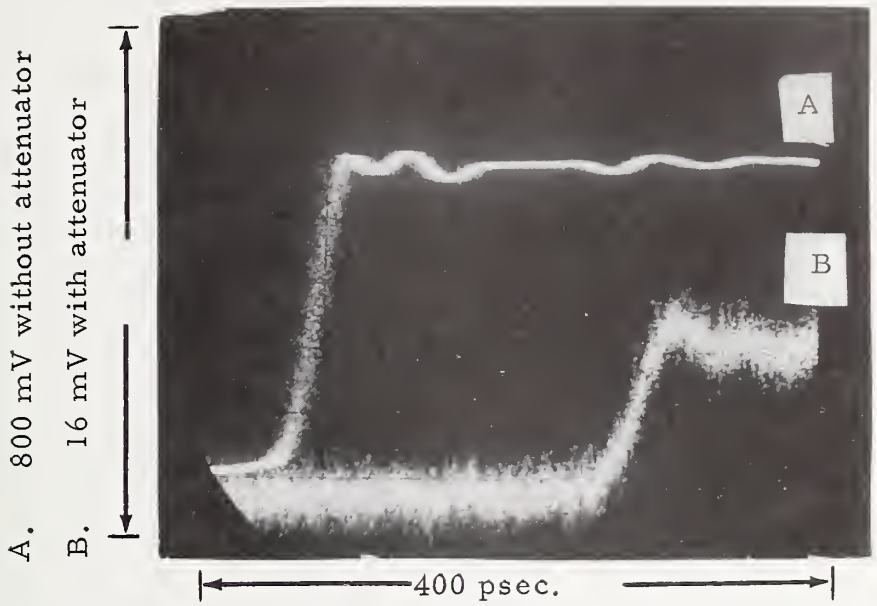


Figure 2-13. Photograph of $e_{d1}(t)$ and $e_{d2}(t)$ for the 40 dB attenuator as seen on the sampling oscilloscope.

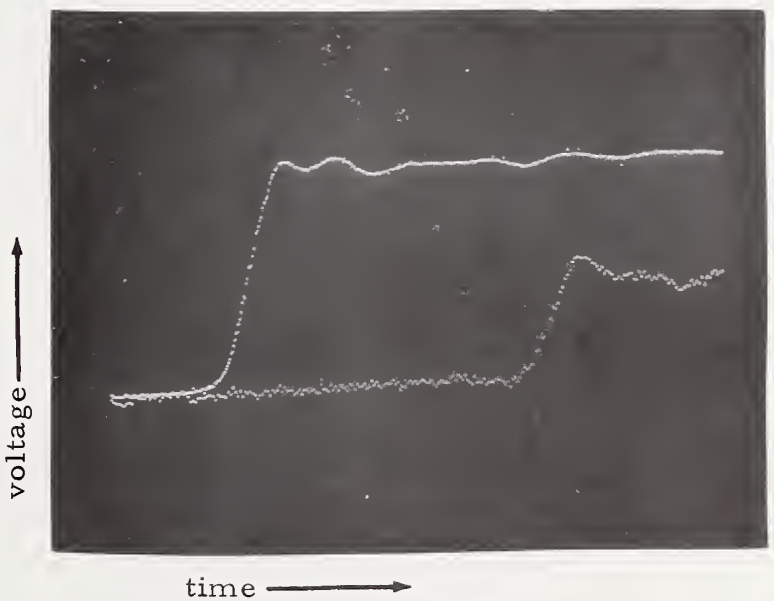


Figure 2-14. Photograph of $e_{d1}(t)$ and $e_{d2}(t)$ for the 40 dB attenuator after signal averaging.

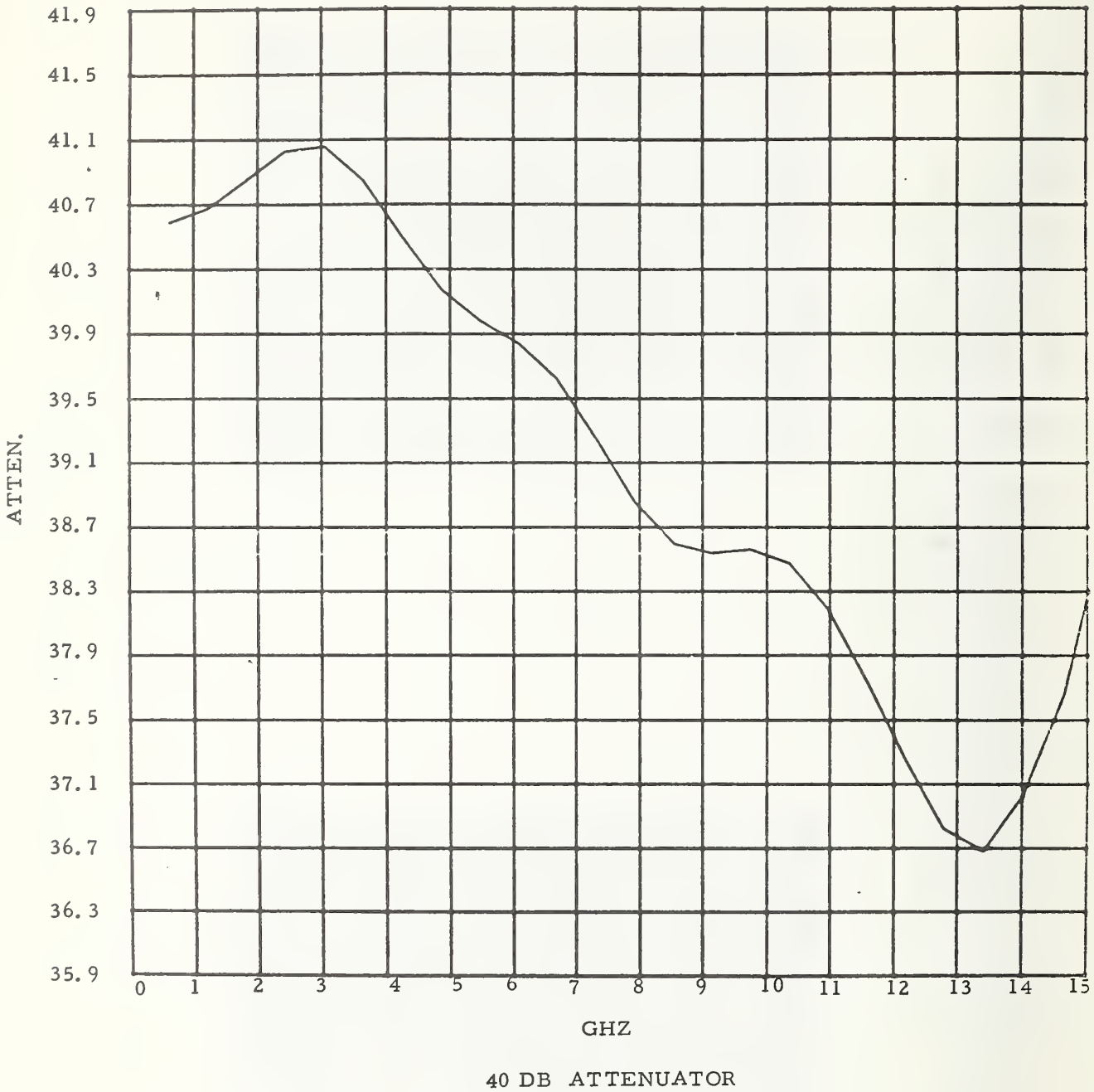


Figure 2-15. Computer plot of the amplitude frequency response of the 40 dB attenuator.

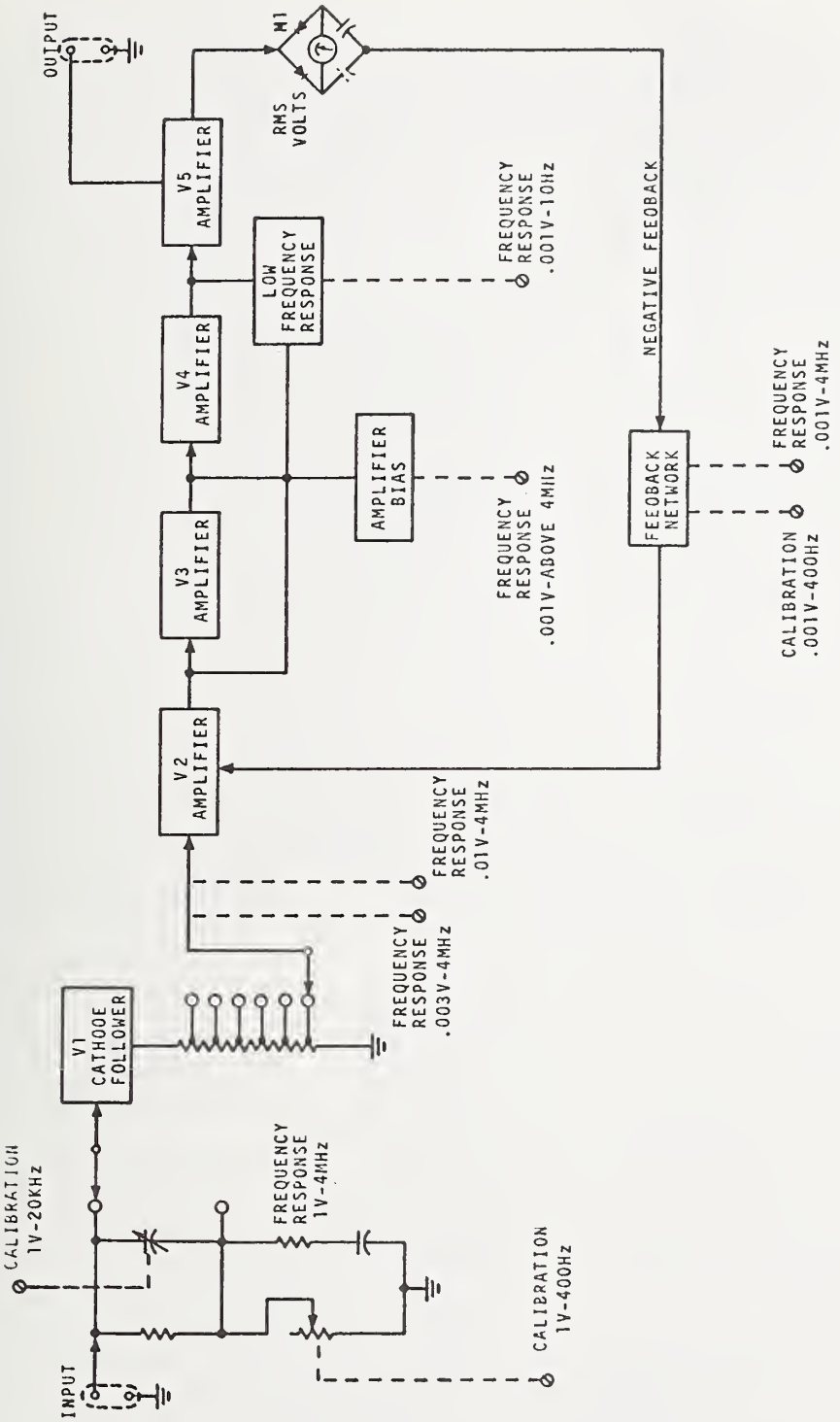


Figure 3-1. Simplified block diagram of ac VTVM tested.

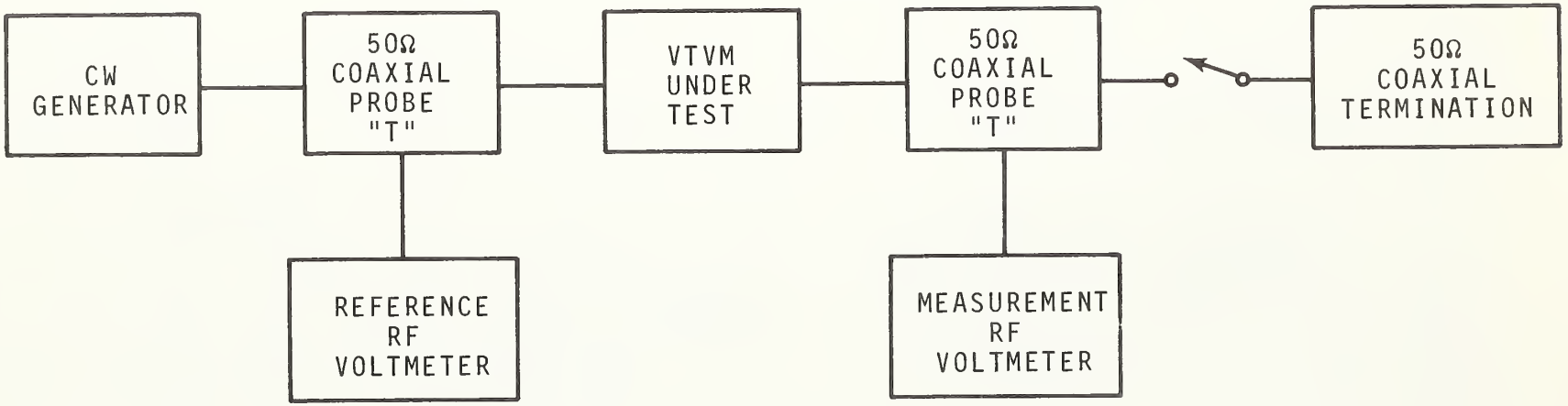


Figure 3-2. Block diagram of system used to perform ac VTVM frequency-domain measurements

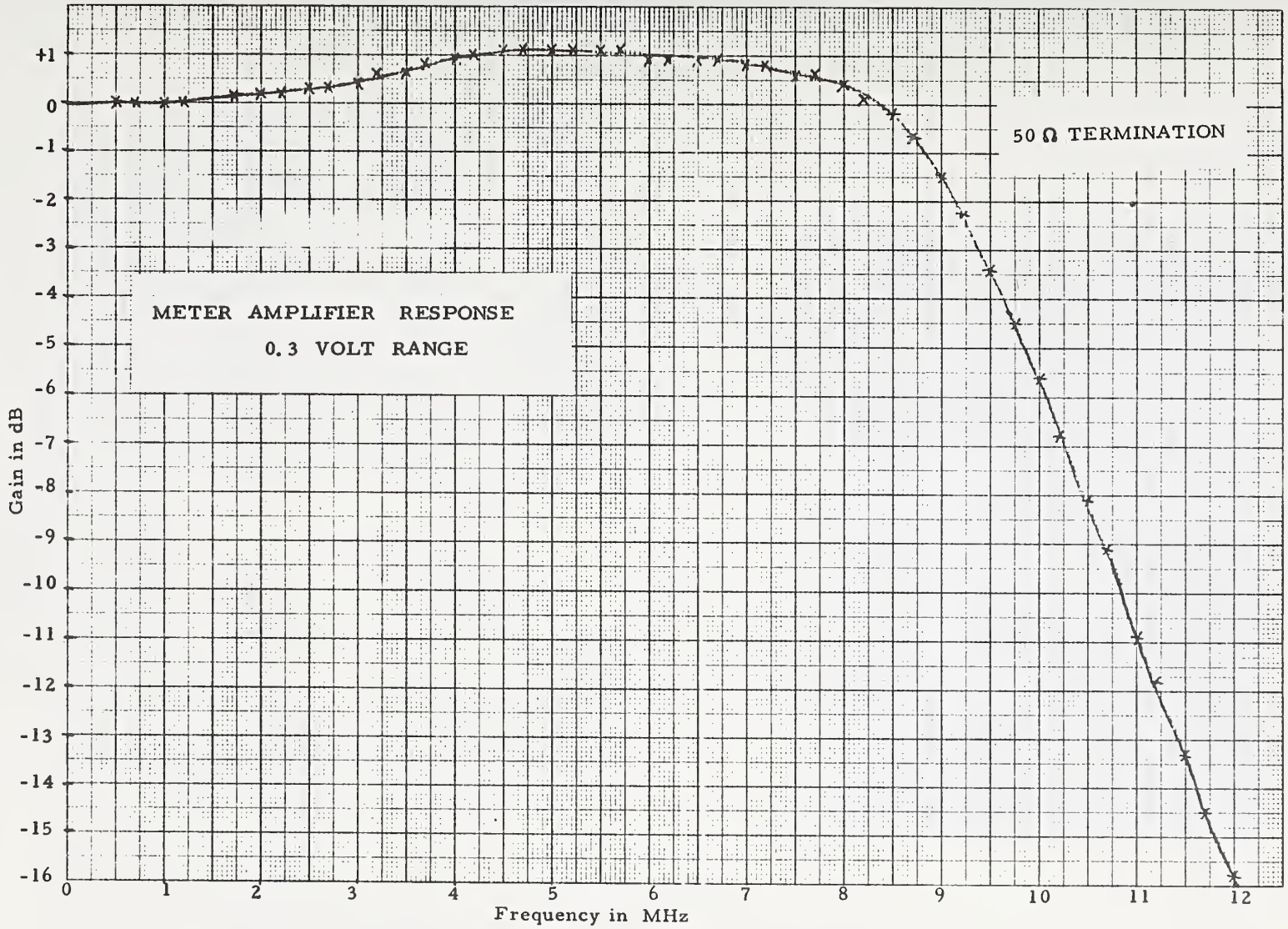


Figure 3-3. Graph of amplitude frequency response of ac VTVM using the 50 Ω termination.

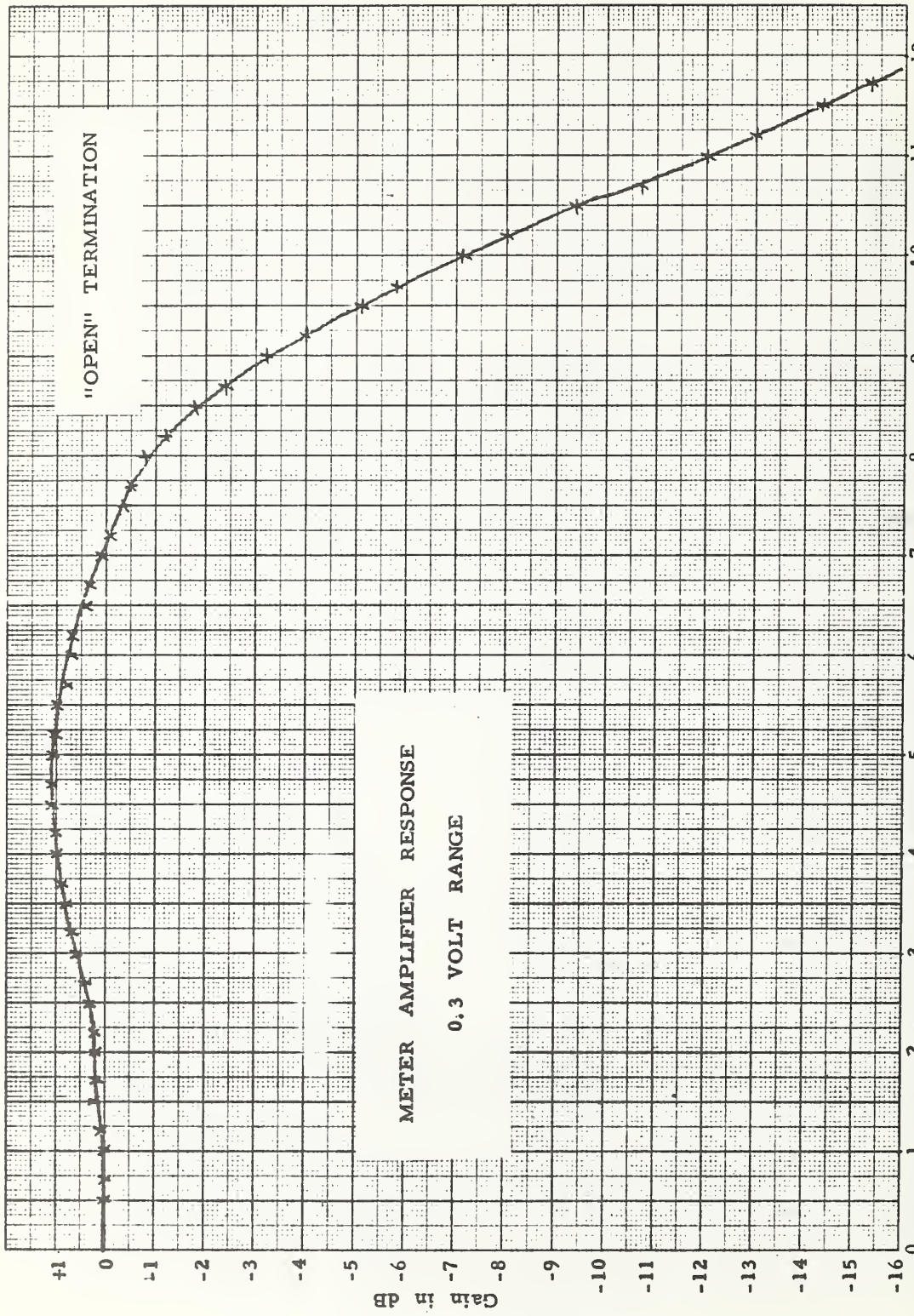


Figure 3-4. Graph of amplitude frequency response of ac VTVM with 50 Ω termination removed.

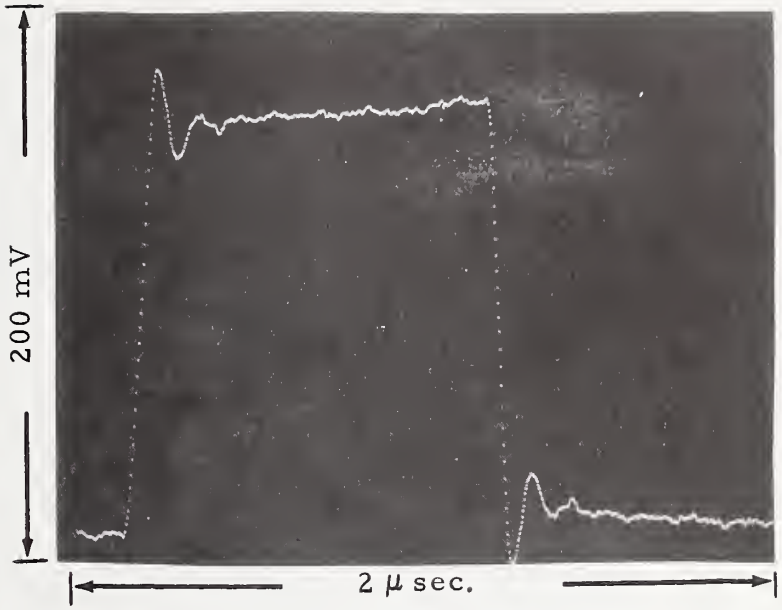


Figure 3-5. Photograph of ac VTVM meter amplifier response waveform after being made periodic and smoothed.

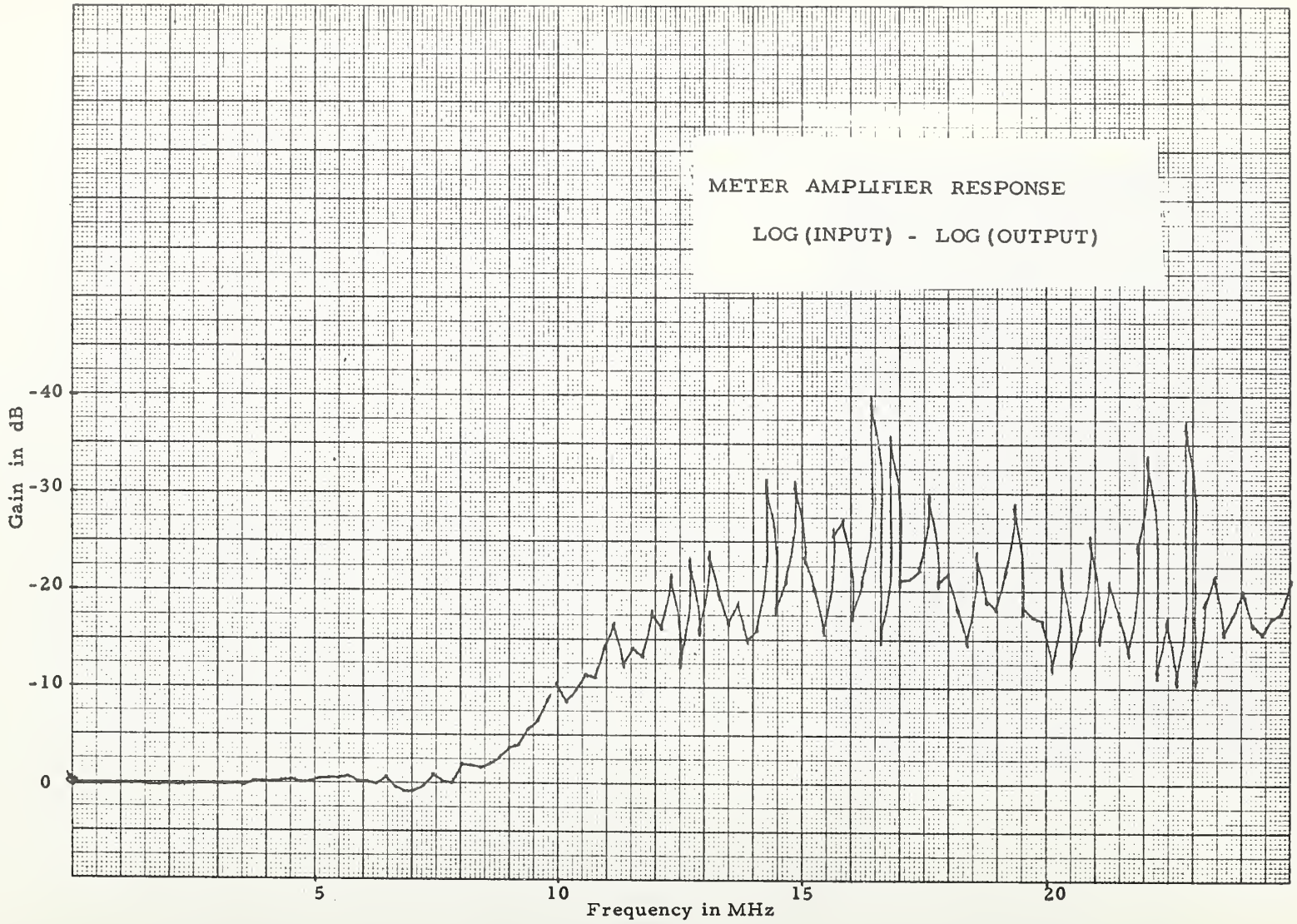


Figure 3-6. X-Y recording of ac VTVM meter amplifier frequency response.

FORM NBS-114A (1-71)

| U.S. DEPT. OF COMM. BIBLIOGRAPHIC DATA SHEET | 1. PUBLICATION OR REPORT NO. NBSIR 73-325 | 2. Gov't Accession No. | 3. Recipient's Accession No. |
|---|---|---|---|

4. TITLE AND SUBTITLE

PULSE TESTING OF RF AND MICROWAVE COMPONENTS

5. Publication Date: July 1973

6. Performing Organization Code

7. AUTHOR(S) William L. Gans and N. S. Nahman

8. Performing Organization

9. PERFORMING ORGANIZATION NAME AND ADDRESS

NATIONAL BUREAU OF STANDARDS, Boulder Labs.
DEPARTMENT OF COMMERCE
Boulder, Colorado 80302

10. Project/Task/Work Unit No. 2725390

11. Contract/Grant No.

12. Sponsoring Organization Name and Address

DoD/CCG

13. Type of Report & Period Covered: Interim Report

14. Sponsoring Agency Code

15. SUPPLEMENTARY NOTES

16. ABSTRACT (A 200-word or less factual summary of most significant information. If document includes a significant bibliography or literature survey, mention it here.)

This interim report is concerned with the application of time domain measurements to the determination of frequency domain parameters. The theory is developed for the calculation of the parameter $S_{21}(\omega)$ from time domain insertion measurements.

Experimental results are presented for a 4.1 GHz low pass filter and coaxial attenuators of 10 dB, 20 dB and 40 dB. Also presented is an experimental justification showing the lack of feasibility of applying time domain techniques to the frequency response calibration of certain ac VTVMs.

17. KEY WORDS (Alphabetical order, separated by semicolons)
Fast fourier transform; frequency response; microwave; pulse; S-parameter; time domain; transfer function

18. AVAILABILITY STATEMENT

☐ UNLIMITED.

☒ FOR OFFICIAL DISTRIBUTION. DO NOT RELEASE TO NTIS.

19. SECURITY CLASS (THIS REPORT): UNCLASSIFIED

21. NO. OF PAGES

20. SECURITY CLASS (THIS PAGE): UNCLASSIFIED

22. Price